# Systematic transcriptome-based comparison of cellular adaptive stress response activation networks in hepatic stem cell-derived progeny and primary human hepatocytes

Braak, B. ter; Niemeijer, M.; Boon, R.; Parmentier, C.; Baze , A.; Richert. L.; ... ; Water, B. van de

Toxicology in Vitro 73 (2021) 105107

Contents lists available at ScienceDirect

Toxicology in Vitro

journal homepage: www.elsevier.com/locate/toxinvit

# Systematic transcriptome-based comparison of cellular adaptive stress response activation networks in hepatic stem cell-derived progeny and primary human hepatocytes

Bas ter Braak [a,1], Marije Niemeijer [a,1], Ruben Boon [b], Céline Parmentier [c], Audrey Baze [c], Lysiane Richert [c], Suzanna Huppelschoten [a], Steven Wink [a], Catherine Verfaillie [b], Bob van de Water [a,*]

[a] Division of Drug Discovery and Safety, Leiden Academic Centre for Drug Research, Leiden University, Leiden, the Netherlands
[b] Department of Development and Regeneration, Stem Cell Institute, KU Leuven, Leuven, Belgium
[c] KaLy-Cell, Plobsheim, France

ARTICLE INFO

*Keywords:*
Induced pluripotent stem cell derived hepatocytes
Oxidative stress
DNA damage
Unfolded protein response
Inflammation
Transcriptomics

ABSTRACT

Various adaptive cellular stress response pathways are critical in the pathophysiology of liver disease and drug-induced liver injury. Human-induced pluripotent stem cell (hiPSC)-derived hepatocyte-like cells (HLCs) provide a promising tool to study cellular stress response pathways, but in this context there is limited insight on how HLCs compare to other in vitro liver models. Here, we systematically compared the transcriptomic profiles upon chemical activation in HLCs, hiPSC, primary human hepatocytes (PHH) and HepG2 liver cancer cells. We used targeted RNA-sequencing to map concentration transcriptional response using benchmark concentration modeling for the various stress responses in the different test systems. We found that HLCs are very sensitive towards oxidative stress and inflammation conditions as corresponding genes were activated at over 3 fold lower concentrations of the corresponding pathway inducing compounds as compared to PHH. PHH were the most sensitive model when studying UPR related effects. Due to the non-proliferative nature of PHH and HLCs, these do not pose a good/sensitive model to pick up DNA damage responses, while hiPSC and HepG2 were more sensitive in these conditions. We envision that this study contributes to a better understanding on how HLCs can contribute to the assessment of cell physiological stress response activation to predict hepatotoxic events.

## 1. Introduction

Drug-induced liver injury (DILI) is one of the most frequent causes for drug withdrawal and the leading cause for compound attrition in drug development (Kullak-Ublick et al., 2017). Current models that are used in drug safety screening include hepatoma cell lines and primary human hepatocytes (PHH), but these models have their limitations. The gold standard for toxicity testing, PHH, have a lack in bioavailability, high cost, high inter-donor variability and tendency to quickly dedifferentiate upon plating. Moreover, they can only provide limited mechanistic information (Lu et al., 2015). HepG2, a liver carcinoma cell line, displays many phenotypic features of normal liver cells, but has a low metabolic capacity compared to PHH. On the other hand, current models that possess relatively high metabolic capacity such as HepaRG and Upcyte, show lower hepatotoxicity predictivity than HepG2 cells in comparison to PHH (Sison et al., 2017).

A new and very promising source for unlimited, stabile cells with potentially improved predictivity for hepatotoxicity are stem cell-derived hepatocyte models (Helsen et al., 2016; José et al., 2016). Ethical issues with embryonic stem cell-derived hepatocytes were

*Abbreviations:* AAT, anti-alpha trypsin; aFGF, acidic fibroblast growth factor,; AIC, Akaike's information criterion,; BMC, benchmark concentration; CPT, cisplatin; DDR, DNA damage response; DEM, diethyl maleate; HGF, hepatocyte growth factor; DILI, drug-induced liver injury; hiPSC, human-induced pluripotent stem cells; HLCs, hepatocyte-like cells; HNF4α, hepatocyte nuclear factor 4 alpha; LDM, liver differentiation medium; NAFLD, non-alcoholic fatty liver disease; PC, principal component; PCA, principal component analysis; PHH, primary human hepatocytes; TNF, tumor necrosis factor α; TUN, tunicamycin..

* Corresponding author: Einsteinweg 55, 2333, CC, Leiden, the Netherlands.
*E-mail address:* b.water@lacdr.leidenuniv.nl (B. van de Water).

[1] Contributed equally to this study.

https://doi.org/10.1016/j.tiv.2021.105107
Received 2 October 2020; Received in revised form 12 January 2021; Accepted 30 January 2021
Available online 3 February 2021

resolved when reprogramming techniques made it possible to generate human-induced pluripotent stem cells (hiPSC) from fibroblasts or any other nucleated somatic cell (Takahashi et al., 2007). This procedure also makes it possible to study hepatotoxicity in patient-derived hiPSC-derived hepatocyte-like cells (HLCs) having specific genetic mutations and drug sensitivity backgrounds (Li et al., 2015). To understand the application value of hiPSC-HLCs as compared to PHH, most studies have measured the expression and activity of biotransformation enzymes, including both phase I, phase II and phase III metabolism, as these are critical components for onset of DILI (Weaver et al., 2019). However, also other cell physiological responses that determine the ultimate fatal outcome for onset of hepatotoxicity are critical to evaluate, including cellular stress response pathways related to either internal or external cues and specific cell injury or inflammatory cytokines. The main cellular stress responses include oxidative stress-mediated NRF2 activation, unfolded protein response (UPR) through ATF4, ATF6 and XBP1 transcriptional responses, DNA damage responses through TP53 signaling and inflammatory cytokine-mediated NF-κB activation (Wink et al., 2018). Most likely, the dynamics and amplitude of these responses differ between cell types and will determine the ultimate cellular outcome. Since various drugs with DILI liability activate these stress pathways (Wink et al., 2018), it is of major interest to compare the cellular stress response pathways between hiPSC-HLCs and PHH. However, so far a systematic analysis of the response of hepatic hiPSC-progeny towards chemically-induced stress is lacking.

Omics approaches, such as transcriptomic profiling, enable a thorough comparison of different liver in vitro models and assess the resemblance to primary hepatocytes or liver tissue. Some studies describe a transcriptomic comparison between HLCs and other models like PHH and hepatoma lines (Gao and Liu, 2017; Godoy et al., 2015), but a comparison of cellular stress responses has not been performed. Recent advances in higher throughput targeted RNA-sequencing technology, such as TempO-Seq, enables a snapshot of the transcriptomic profiles of thousands of genes for various conditions (Ramaiahgari et al., 2019; Yeakley et al., 2017). This allows for detailed concentration response evaluation of chemical-induced cell injury responses in various cell types. Here using the TempO-Seq technology, a cost-effective technique allowing for the evaluation of the expression of a targeted set of genes only needing a small amount of sample, we compared the chemically-induced cellular stress response activation in hiPSC-HLCs with cryopreserved PHH and HepG2 cells. We used diethyl maleate to induce an oxidative stress response, tunicamycin to induce unfolded protein stress response, cisplatin to induce the DNA damage response and tumor necrosis factor alpha (TNFα) to initiate inflammatory cytokine signaling for 8 h to capture the primary stress response activation. The goal of this study is to compare specific stress pathway activation sensitivities to evaluate the suitability of each model in a hepatotoxicity assay. To our knowledge, this is the first systematic study that focusses on the transcriptomic effect of chemically-induced cellular stress responses in hiPSC-derived hepatocytes.

## 2. Materials and methods

### 2.1. Cell culturing

The hiPSC BJ-1 line (generated at KU Leuven) was cultured on Matrigel (Corning) coated plates. Medium (mTeSR1) was refreshed daily. Full description of the characteristics of the hiPSC BJ-1 line can be found in Helsen et al. (Helsen et al., 2016). The human liver carcinoma cell line, HepG2, obtained from American Type Culture Collection (ATCC) were cultured as described in Wink et al. (Wink et al., 2014). Cryo-preserved PHH derived from three different individuals (S1295T: 86-year-old male Caucasian patient with hepatocellular carcinoma; S1307T: male Caucasian 75-year-old patient with colorectal carcinoma; and S1423T: male Caucasian 68-year-old patient with colorectal adenocarcinoma) were provided by KaLy-Cell (Plobsheim, France) and selected based on their plateability. PHH were thawed, transferred to pre-warmed thawing UCRM medium (IVAL, Columbia, USA), transferred to pre-warmed seeding UPCM medium (IVAL). Viability was assessed using the Trypan Blue, cells were seeded at a density of 70.000 viable cells per well in 96 wells Biocoat Corning Collagen I Cellware plates from Corning (Wiesbaden, Germany). Medium was refreshed using seeding UPCM medium 6 h after plating. Compound exposures were done 24 h after plating in William's E medium supplemented with 100 U/mL penicillin and 100 μg/mL streptomycin.

### 2.2. Differentiation of hiPSCs towards hepatocytes

HiPSCs were differentiated to HLCs as described by Tricot et al. (Tricot et al., 2018). In short, BJ1 hiPSC cells were seeded in mTeSR, supplemented with 1:100 Revitacell (Thermofisher), with 100.000 cells per 48-well. During differentiation, the cells were cultured on liver differentiation medium (LDM). In addition to the growth factors Activin-A (100 ng/mL), Wnt3a (50 ng/mL), BMP4 (50 ng/mL), FGF1 (50 ng/mL), and HGF (20 ng/mL) (Fig. 1a), 0.6% DMSO (Sigma-Aldrich) was added from day 0 until day 11, from day 12 until day 25 2% DMSO was added to the LDM (Tricot et al., 2018). It was shown that DMSO improves the hepatic differentiation by downregulation of pluripotency genes (Czysz et al., 2015). Medium was refreshed daily. All growth factors were purchased from PeproTech. For the biological replicates three different stem cell culture flasks were used, which were differentiated separate from each other.

### 2.3. Cell treatment

Model compounds for oxidative stress (diethyl maleate; DEM) and unfolded protein response (tunicamycin; TUN) were purchased from Sigma-Aldrich, the cytokine to induce an inflammation response (tumor necrosis factor α; TNF) was purchased from R&D systems and the DNA damage response compound (cisplatin; CPT) from Ebewe. For each compound a concentration range was chosen that is known to induce the corresponding stress pathway without inducing cytotoxicity (Fredriksson et al., 2014; Liguori et al., 2005; Wink et al., 2018). Prior to exposure, 1000 times concentrated stock solutions were made in DMSO (DEM, TUN) or PBS (TNF, CPT). Exposures were performed by adding 100 μL two times concentrated exposure medium (with 0.2% DMSO independent of compound exposure) to each well already containing 100 μL maintenance medium. Cells were exposed for 8 h in a 5% $CO_2$ humidified incubator at 37 °C. Thereafter, cells were washed with PBS, lysed with 1× TempO-Seq lysis buffer, stored at −80 °C and shipped for targeted sequencing. All exposure experiments have been performed with three independent biological replicates using different compound stock solutions.

### 2.4. Immunofluorescence

Maturity status of the HLC differentiation was assessed with immunofluorescence using hepatocyte markers HNF4α (1:200, Abcam, ref. #ab41898) and AAT (1,200, Dako, ref.#A0012) following the protocol described in Boon et al. (Boon et al., 2020).

### 2.5. Targeted sequencing

Gene expression profiles were analyzed using a targeted RNA sequencing technology, TempO-Seq (Biospyder Technologies, Inc., Carlsbad, CA, USA). A set of genes was selected based on the S1500+ gene list of NIEHS (Mav et al., 2018). This list contains 2736 genes that provide maximal toxicogenomic information on chemical perturbations that reflect general cellular responses. We supplemented this list with another 245 genes that are involved in hiPSC to hepatocyte differentiation, cellular stress pathways activated in PHH (Fredriksson et al., 2014) and were missing in the S1500 list (for complete gene list see

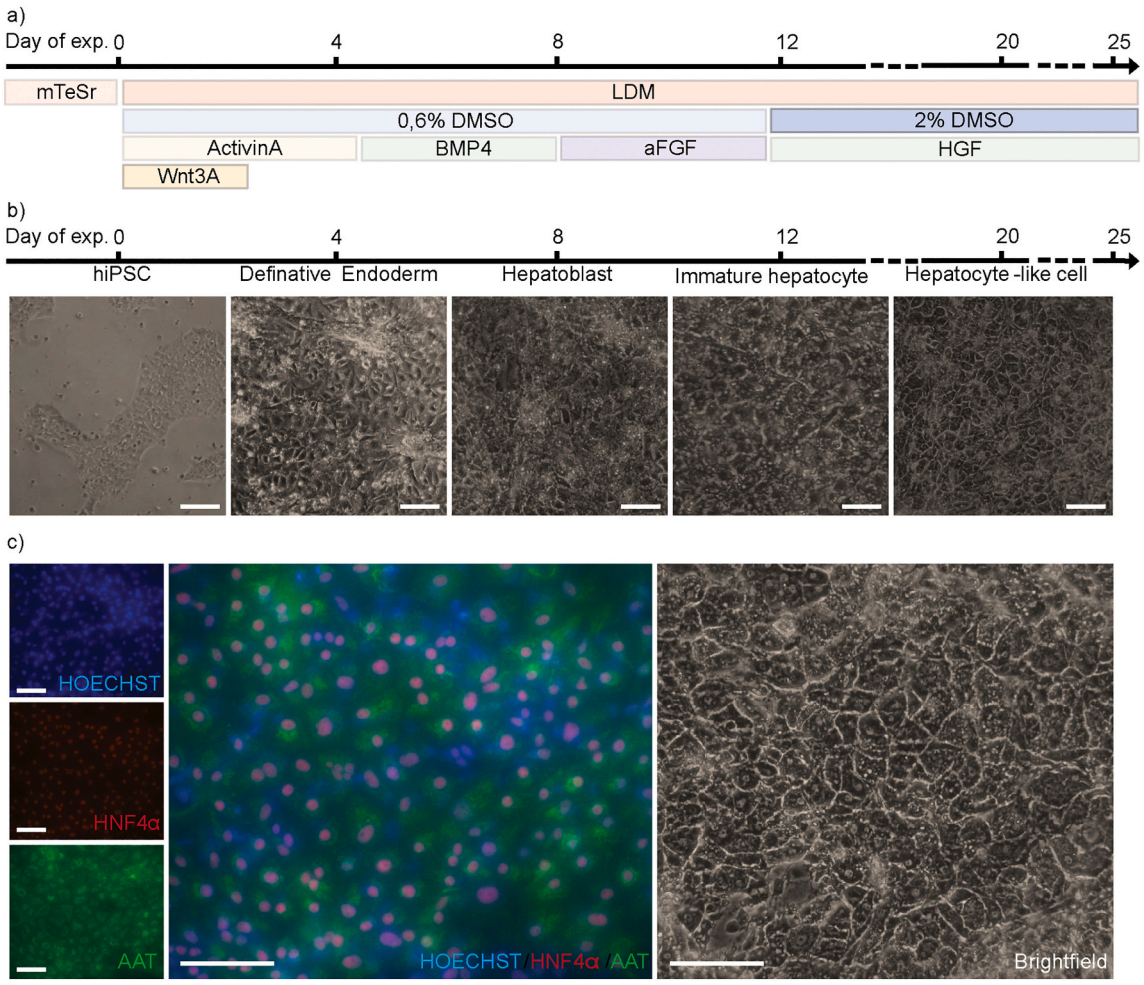


**Fig. 1. HiPSC-hepatocyte differentiation process and differentiation quality**. A) The 25-day hiPSC-HLC differentiation mTeSR based protocol. Compound exposures were performed at the indicated days during differentiation (0, 4, 8, 12, 20 and 25 days). B) Brightfield image overview of the differentiation process, in which several intermediate cell types can be identified. C) Immunofluorescence (HNF4α and AAT) and brightfield imaging of hepatocyte-like cells (day 25). Scale bars represent a size of 100 μm.

ESM1). A detailed description of the sample processing was described by Yeakley et al. (Yeakley et al., 2017). In short, mRNA in the lysates was hybridized with detector oligo mix, and amplified using barcoded primer pairs to add a unique tag for each of the samples. Sample amplicons were pooled and purified. The libraries were sequenced using a HiSeq 2500 Ultra-High-Throughput Sequencing System (Illumina, San Diego, CA). De-multiplexing of the sequencing readouts resulted in FASTQ files.

### 2.6. Data processing

TempO-seq transcriptomics derived reads were aligned using the TempO-seqR package (done in-house by BioSpyder Technologies). Raw counts were normalized using the DESeq2 R package and log2 transformed. A library size (sum of reads within one sample) cut-off was used of 100.000 reads. Samples that did not meet this criterion were excluded for further analysis. Replicate Pearson correlation was calculated for each condition and model (supplemental figure ESM5). Data has been uploaded to the Gene Expression Omnibus (GEO) with series accession number GSE155771. Benchmark concentration (BMC) modeling was done using the BMDExpress 2 software (developed by Sciome LCC and NIEHS/NTP/EPA) to assess difference in sensitivity (Phillips et al., 2019). Here, the dose responses were fitted with various continuous models (exponential, linear, polynomial, hill and power model) for each gene and sample. Best model was selected which had the lowest Akaike's information criterion (AIC) (Kadota et al., 2015) and a $p$-value of $>0.05$. The BMC was defined as the concentration at 1 standard deviation increase of gene expression. Genes were considered significant differentially expressed across dose-response when the adjusted p-value was $<0.05$ using a Williams trend test and Benjamini & Hochberg post-hoc test. Principal Component Analysis (PCA) of the log2 normalized counts or fold changes was done using the prcomp function from the Stats R package. Besides BMDExpress 2, Rstudio version 1.0.153 (Boston, USA) in combination with R 3.4.1 was used for data analysis including the following R packages: DESeq2 (Love et al., 2014), AnnotationDbi (Pagès et al., 2018), pheatmap (Kolde, 2012), ggplot2 (Wickham, 2009), data.table (Dowle et al., 2016)), dplyr (Wickham, 2011), tidyr (Wickham and Henry, 2018), reshape2 (Zhang, 2016), scales and stats. Using R package pheatmap, hierarchical clustering of pathway-related genes was done based on Euclidean distance of log2 fold changes using Wards method.

### 2.7. Retrieving pathway specific gene list

To examine stress response perturbations by each compound using PCA, genes were selected when the mean maximal fold change across the dose response for the three PHH donors was higher than 4 for DEM, TUN and CPT, and 3.5 for TNF treated cells (for gene lists see ESM2). For hierarchical clustering and BMC distribution plots, stress response pathway-related genes were based on target genes of stress response

specific transcription factors (UPR: *ATF4*, *ATF6*, *XBP1* and *DDIT3*; OX: *NFE2L2*; DDR: *TP53*; Inflammation: *RELA*, *REL* and *NFKB1*) defined by DoRothEA v2 (Garcia-Alonso et al., 2018) with confidence level of A to D which were present in the S1500+ geneset. Of these genes, the top 30 were selected based on the rank of both maximal fold change across dose and BMC having at least a fold change of 2.5 for one of the cell types (for gene lists see ESM3). These genes were used for hierarchical clustering and BMC distribution comparison to assess sensitivity for pathway activation. To evaluate the specificity of the compounds activating the stress responses of interest, we have performed transcription factor activity analysis using gene set enrichment analysis using the viper R package of the transcription factor regulons defined by DoRothEA vs with a confidence level A to D present in the S1500+ geneset. Transcription factors were filtered based on FDR $< 0.05$ and the top 20 were selected based on ranking of the minimum FDR across concentration range having a positive NES.

## 3. Results

### 3.1. HiPSC differentiation to hepatocyte-like cells

A twenty day hiPSC-hepatocyte differentiation protocol (Tricot et al., 2018) was followed (Fig. 1a), in which growth factors ActivinA and Wnt3A started the hiPSC differentiation process towards a definitive endoderm cell stage (Fig. 1b). At this point the cells showed a typical epithelial morphology and stopped proliferating. Addition of bone morphogenetic protein 4 (BMP4) differentiated these cells further towards hepatoblasts followed by a 4-day long stimulation with acidic fibroblast growth factor (aFGF) which resulted in immature hepatocytes. In the last phase of the differentiation protocol, hepatocyte growth factor (HGF) was added to the LDM which resulted in cells with a typical cuboidal morphology (Acikgöz et al., 2013), that stained positive for anti-alpha trypsin (AAT) and hepatocyte nuclear factor 4 alpha (HNF4α) (Fig. 1c).

### 3.2. Transcriptomic overview of the differentiation process and comparison to PHH and HepG2

To assess the shift in the gene expression profile during the differentiation process, gene expression levels of undifferentiated hiPSC were compared with the different hepatocyte-differentiation stages and compared to HepG2 and the gold standard PHH, all in basal/unexposed conditions. General transcriptomic profiles between different cell types were compared using a principle component analysis (PCA). A relatively small difference was seen when hiPSCs were differentiated towards HLCs compared to PHH in the first principal component (PC) explaining 54.3% of the variance (Fig. 2a), and they remained co-localized with HepG2 cells but not PHH. The liver associated genes, such as Haptoglobin (*HP*), Albumin (*ALB*) and Orosomucoid 1 (*ORM1*), were chiefly responsible for the relatively small shift towards PHH. In PC2, a significant difference could be seen between hiPSC and HLCs, which was mostly accounted for by the enormous upregulation of both immature liver specific genes during differentiation, including alpha-fetoprotein (*AFP*), and mature liver specific pre-albumin Transthyretin (*TTR*),

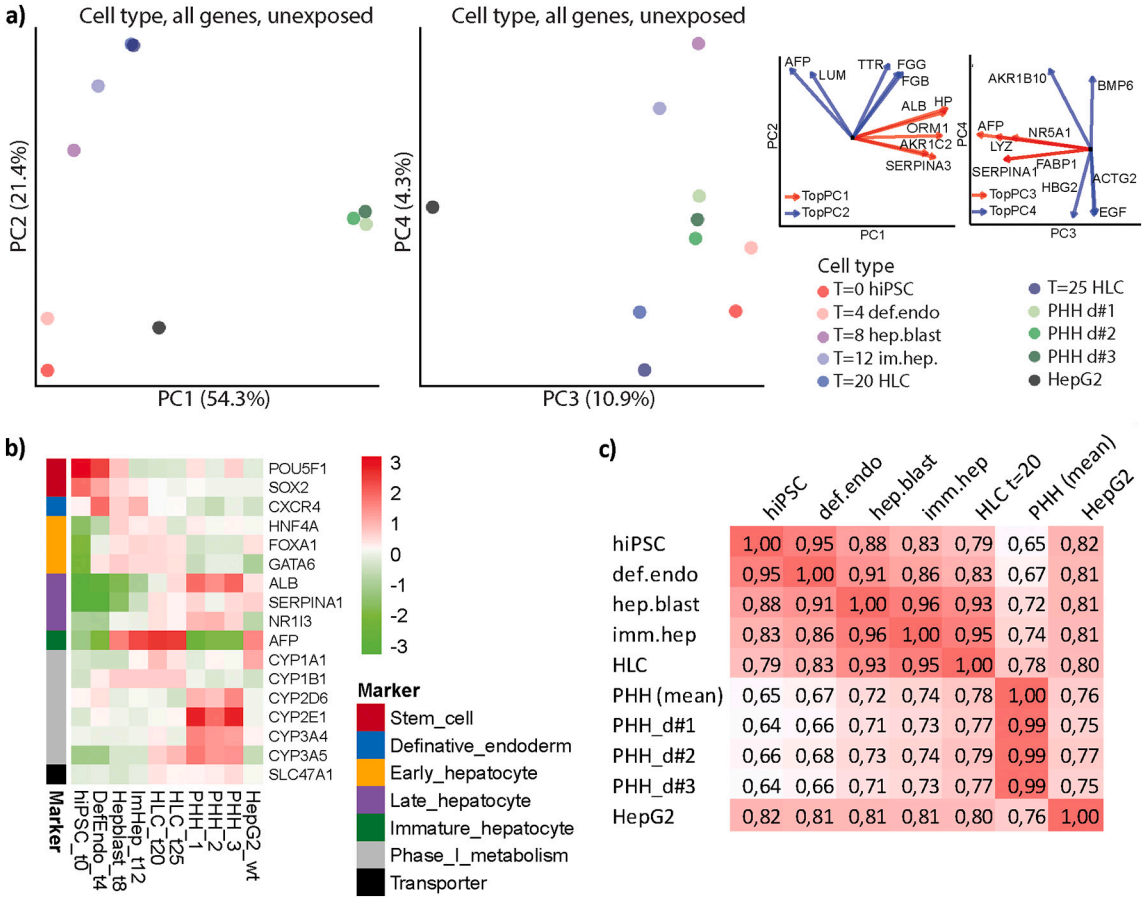


**Fig. 2. Transcriptomic analysis of the hiPSC-hepatocyte differentiation process benchmarked to PHH and HepG2.** A) Principle component analysis (PCA) of all genes at basal conditions of the different cell types using log2 transformed counts. The top 5 genes most determining the corresponding principle components are depicted on the right, where red arrows represent genes most affecting the principle component on the x-axis and blue on the y-axis. B) Heat map of the log10 FC expression levels of differentiation markers during hiPSC-hepatocyte differentiation process, the fold changes are compared to the median expression of each gene. C) Pearson correlation matrix on normalized gene expression counts of the different cell types. $N = 3$.

Fibrinogen Beta Chain (*FGB*) and Fibrinogen Gamma Chain (*FGG*). The biological variation between the different hiPSC progeny steps was relatively small as a clear separation of the different cell differentiation stages and cell types could be observed. hiPSC-hepatic progeny moved along the axis of PC4 and addition of BMP4 in the first 8 days of differentiation induced a strong *BMP6* expression, which was lost from day 9 onward. In addition, expression of Hemoglobin Subunit Gamma 2 (*HBG2*), a gene highly expressed in immature hepatocytes, was significantly upregulated. The variation between the different PHH donor populations was relatively small in all PCs. Interestingly, in PC3, a clear separation of HepG2 from all other cells became evident, primarily driven by high expression of *AFP* and Lysozyme (*LYZ*) in this cell line.

Next, we evaluated the expression of well-known markers for each hiPSC differentiation stage. The stem cell markers *POU5F1* and *SOX2* were highly expressed in undifferentiated hiPSC stage, but as expected were downregulated by >1000-fold upon differentiation towards HLCs (Fig. 2b). At step 1 of differentiation, the definitive endoderm marker *CXCR4* was more than 50-fold increased. Early hepatocyte markers *FOXA1* and *HNF4α* were highly induced in the HLC stage and reached expression levels similar to those in PHH (Ghosheh et al., 2016; Godoy

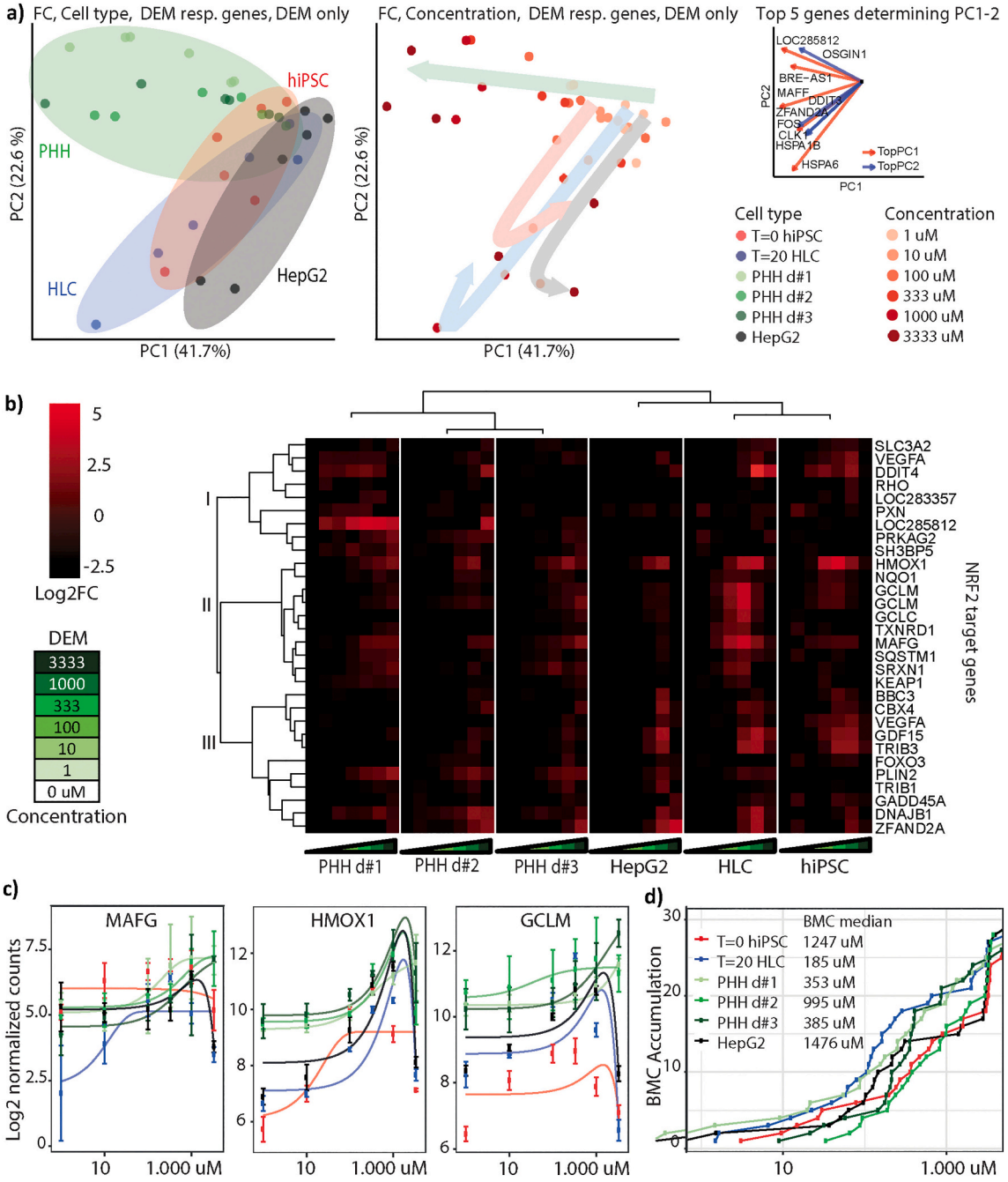


**Fig. 3. Effect of oxidative stress on the transcriptomic space of hiPSC, HLC, PHH and HepG2.** A) Left panel: PCA of log2 normalized counts of DEM responsive genes with all treatments. Right panel: PCA of log2 fold changes of the DEM responsive genes after DEM exposure. The vector plots on the right represent the top 5 most determining genes of PC1 (red) or PC2 (blue). The size and orientation of the vector represent the contribution and PC-orientation of the 10 genes. B) Hierarchical clustering of the log2 fold changes of the top 30 responding oxidative stress genes after DEM exposure. C) Concentration response curves of log2 normalized counts for three oxidative stress genes after DEM exposure. Dots and error bars (SE) represent gene expression data, lines represent best BMC model. D) BMC accumulation plots of the top 30 responding oxidative stress genes after DEM exposure. Median BMC were extracted from these plots. $N = 3$.

et al., 2015). *AFP*, a gene that is associated with fetal hepatocytes, was highly expressed in HLCs suggesting an immature hepatocyte phenotype. Late hepatocyte markers, such as *ALB, NR1I3* and *SERPINA1* were strongly induced during the differentiation process, where transcript levels for *NR1I3* and *SERPINA1* levels were comparable to PHH. However, *ALB* gene expression levels remained still >10-fold lower compared to PHH. A key feature of hepatocytes is their ability to metabolize drugs. Phase 1 metabolism is mainly regulated by Cytochrome P450 (CYP) enzymes. During differentiation some of these enzymes (e.g. *CYP1A1, CYP1B1,* and *CYP3A5*) were strongly induced and reached similar or higher expression levels as compared to PHH. Several other enzymes including *CYP2D6, CYP2E1* and *CYP3A4* remained significantly less expressed in HLCs as compared to PHH, indicating the immaturity of the HLCs. For metabolically functional hepatocytes, expression of transporters is necessary, especially *SLC47A1* plays an important role in xenobiotic clearance (Lundquist et al., 2014). In contrast to HepG2, the SLCs were expressed at a similar level in HLCs as compared to PHH. Thus, as summarized in Fig. 2C, the gene expression profiles of the differentiated hiPSCs correlated increasingly stronger with PHH, with hiPSC:PHH correlation of 0.65 and HLC:PHH correlation of 0.78. The correlation of HepG2:PHH was 0.76. The variation along the different donors of PHH was relatively small as all had a correlation of 0.99 with the mean of the PHH.

### 3.3. Transcriptomic space of HLCs and other models in oxidative stress conditions

Diethyl maleate (DEM) is an electrophilic compound which conjugates with cysteine residues in KEAP1 thus activating the activation of the NRF2 pathway, and at higher concentration also affecting the levels of reduced glutathione, thereby disturbing the cellular redox balance and allowing oxidative stress (Kaur et al., 2006). DEM was used as a model compound to induce an overall cellular oxidative stress response. A selection of DEM upregulated genes was based on having a minimum fold change of 4 across dose response of DEM in PHH (see ESM2 for complete list). We performed a PCA analysis on the fold changes DEM vs DMSO to examine the effect on gene expression of the DEM responsive genes (Fig. 3a). Interestingly, at the lowest DEM concentrations all cell types co-localized in the PCA plot, indicating similar behavior between cell types under mild oxidative stress conditions. A very clear DEM concentration-dependent shift in PC1 could be detected for PHH and HLCs, and to a lesser extent hiPSC and HepG2. This effect was predominantly caused by increasing expression of heat shock proteins (secondary response after oxidative stress) or one of the downstream targets of the NRF2 pathway (*MAFF*). Interestingly, at the highest DEM concentration the samples shifted up again on the PC2 axis indicating a downregulation of the NRF2 pathway. The DEM concentration-dependent shift of PHH moved along the PC1 axis which was mainly related to the high expression of the NRF2 target gene oxidative stress induced growth inhibitor 1 (*OSGIN1*) gene.

Next, we investigated the top 30 most responding oxidative stress genes after DEM exposure. Genes were selected on the basis of direct targets of NRF2 as defined by DoRothEA v2 (Garcia-Alonso et al., 2018). Activation of transcription factors was evaluated by gene set enrichment analysis of the transcription factor downstream targets (supplemental table ESM4), where among *NFE2L2* also *ATF4*, important in the UPR, was activated among the models. Hierarchical clustering of NRF2 genes based on Euclidean distance identified genes involved in secondary cell stress responses (e.g. *FOXO3, DNAJB1, TRIB3*) in cluster III and genes involved in the NRF2 mediated oxidative stress response (e.g. *HMOX1, SRXN1, KEAP1, MAFG, GCLM, GCLC, NQO1*) in cluster II (Fig. 3b). Especially in cluster II, HLCs appeared to be more responsive towards DEM as compared to the hiPSC, PHH and HepG2. Clustering of the models indicated that the oxidative stress gene expression profiles of HLCs are similar to hiPSC having higher induction at lower concentrations as compared to PHH.

To further investigate the pathway specific sensitivity of each model, a BMC analysis was performed (Fig. 3c) where the BMC was defined as the concentration at which the target gene expression increases by 1 standard deviation above baseline levels. For this analysis, the same pathway specific top 30 oxidative stress genes were selected. The cumulative BMC plots indicated that hiPSC-derived HLCs were most sensitive towards DEM exposure, having a median BMC of 185 μM (Fig. 3d). PHH were in general less sensitive than HLCs having a median BMC of 353, 385 or 995 μM, and there were significant differences between donors. HepG2 and undifferentiated hiPSCs appeared to be the least sensitive (1476 and 1247 μM, respectively).

### 3.4. Transcriptomic space of different liver test systems for the unfolded protein stress response

Tunicamycin (TUN) was used to induce the UPR as it inhibits N-linked glycosylation thereby disturbing protein folding of glycoproteins leading to ER stress (Wang et al., 2015). A PCA analysis was performed to visualize the transcriptomic changes at the different concentrations of TUN of the different models. We focused the analysis on TUN responsive genes that changed in expression by >4-fold in PHH across the dose response (Fig. 4a; ESM2 for list of genes). The PCA analysis, based on log2 fold changes TUN vs DMSO control, showed that with lower TUN concentrations all models did behave similar (Fig. 4a). Upon increasing concentrations of TUN, all cell types moved up in PC2, which was mainly caused by high levels of expression of *DDIT3, HERPUD1* and *MANF* at increasing concentrations of TUN. These genes are all well known to have a role in the adaptive response against ER stress. Interestingly, four samples moved to the right on the PC1 axis at the highest TUN concentration (100 μM) (HLCs and all three donors of the PHH). This shift was caused by, among others, a downregulation of UPR responding genes and upregulation of early stress response genes (e.g. *FOS* and *EGR1*), indicating that HLCs and PHH were more sensitive towards ER stress than HepG2 and hiPSC. This illustrated a similar TUN dose-response behavior of HLCs and PHH. We also performed hierarchical clustering (Fig. 4b) analysis, including the 30 UPR related genes most affected by TUN exposure. In general, UPR genes were stronger upregulated in HLCs. In HLCs and hiPSCs there was a threshold concentration of TUN when the UPR was started to be induced. Below 1 μM the pathway was inactive but at 1, 10 and 100 μM there was a very pronounced induction. However, for PHH, this effect seemed to be more gradual, starting already at 0.001 μM TUN where there is some upregulation of UPR related genes. Dose response curves of three example and well-known targets of the UPR response (*DDIT3, HERPUD1* and *HSPA5*) demonstrated that basal expression of UPR downstream targets was lower in the HepG2 and hiPSC (Fig. 4c). Transcription factor activity analyses revealed the activation of both UPR related transcription factors, but also NF-κB related transcription factors such as *RELA* and *NFKB1* (supplemental table ESM4). The BMC accumulation plot of the 30 most affected TUN modulated genes showed that PHH are the most sensitive for UPR with considerable variation between different donors (median BMC of 0.02–0.23 μM) (Fig. 4d). Undifferentiated hiPSCs and their differentiated HLC progeny were less sensitive than PHH (median BMC 0.3 and 0.68 μM, respectively). Of note, UPR target genes were only upregulated at much higher concentrations of TUN in HepG2 cells (median BMC of 1.84 μM).

### 3.5. Transcriptomic space of hiPSC-HLCs and other models in DNA damage conditions

Cisplatin (CPT), a clinically relevant anticancer agent, was used to induce a DNA damage response (DDR). CPT induces intra and interstrand DNA adducts, eventually resulting in single and double stranded DNA breaks and subsequent induction of a DDR (Kritsch et al., 2017). Selection of CPT upregulated genes was based on PHH-gene expression after CPT exposure having a minimal fold change of 4

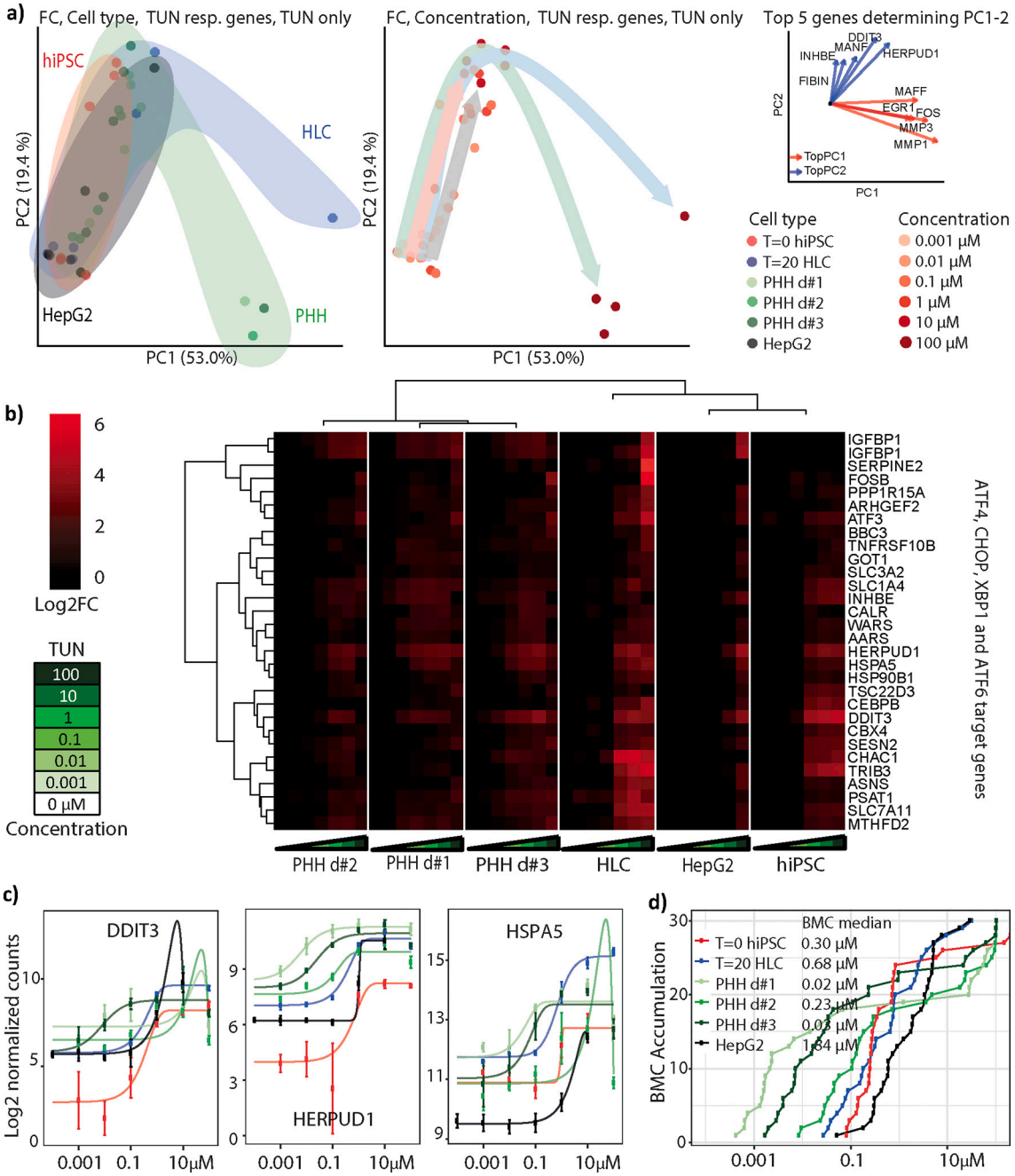


**Fig. 4. Effect of the unfolded protein response on the transcriptomic space of hiPSC, HLC, PHH and HepG2.** A) Left panel: PCA of the unfolded protein genes (log2 normalized counts) with all treatments. Right panel: PCA of log 2-fold changes of the TUN responsive genes after TUN exposure. The vector plots on the right represent the top 5 most determining genes of PC1 (red) or PC2 (blue). The size and orientation of the vector represent the contribution and PC-orientation of the 10 genes. B) Hierarchical clustering of the log2 fold changes of the top 30 UPR related genes after TUN exposure. C) Concentration response curves of log2 normalized counts for three UPR genes after TUN exposure. Dots and error bars (SE) represent gene expression data, lines represent best BMC model. D) BMC accumulation plots of the top 30 responding UPR related genes after TUN exposure. Median BMC were extracted from these plots. $N = 3$.

across dose response (see gene list ESM2). PCA analysis of the log2 fold change of CPT vs DMSO showed that the response of HLCs was most similar to PHH (Fig. 5a). A clear dose response shift could be observed towards high PC2 and low PC1 values. High expression of typical TP53 downstream targets (*MDM2* and *BTG2*) contributed to this shift. The concentration response shift of HLCs and PHH moved more along the PC1 axis compared to hiPSC and HepG2, predominantly caused by increased expression of ATM dependent genes (e.g. *CDK5R1* and *H2AFX*). Interestingly, at the highest concentration of CPT, all 3 PHH donor samples showed a major shift in the PC2 transcriptomic space. A reduction of the typical DNA damage response genes was observed. This indicates a clear tipping point where PHH switch from adaptation to DNA damage towards adverse regulated cell death programs. Apparently, this tipping point is only reached at higher concentrations of CPT in the other models. The hierarchical clustering on the 30 most responsive downstream targets of TP53 after CPT exposure revealed that the gene induction pattern of HLCs, HepG2 and PHH were similar (Fig. 5b), while hiPSC were most distinct. The log2 normalized counts of three DDR genes, *BTG2, GADD45A* and *MDM2*, demonstrated that although the expression profiles were similar for HLCs and PHH, basal expression levels of TP53 downstream targets were much lower in HLCs (Fig. 5c). Furthermore, the tipping point at which PHH switch from

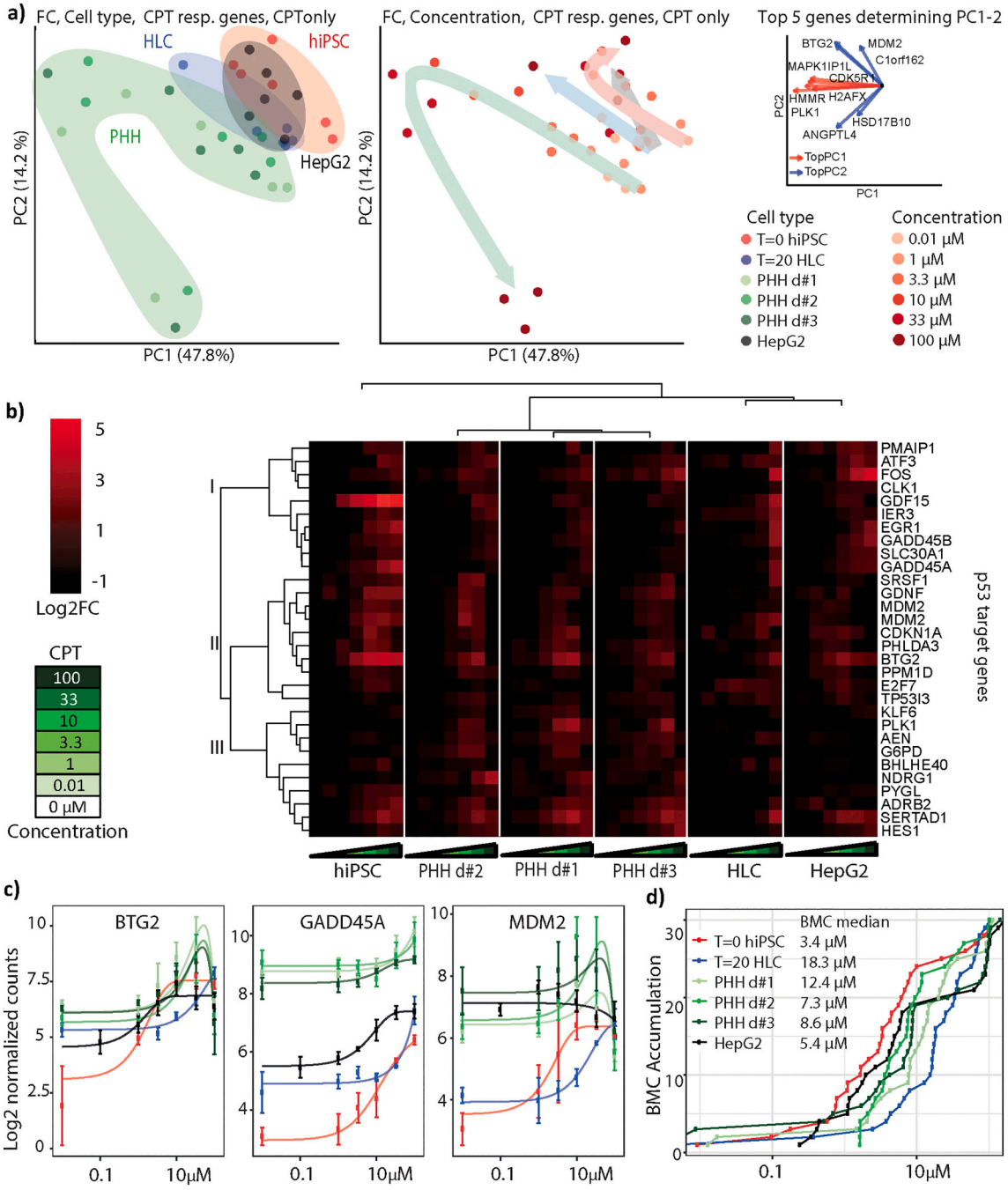


**Fig. 5. Effect of the DNA damage response on the transcriptomic space of hiPSC, HLC, PHH and HepG2.** A) Left panel: PCA of the CPT responsive genes (log2 normalized counts) with all treatments. Right panel: PCA of log2 fold changes of the CPT responsive genes after CPT exposure. The vector plots on the right represent the top 5 most determining genes of PC1 (red) or PC2 (blue). The size and orientation of the vector represent the contribution and PC-orientation of the 10 genes. B) Hierarchical clustering of the log2 fold changes of the top 30 DNA damage response (DDR) related genes after CPT exposure. C) Concentration response curves of log2 normalized counts for three DDR genes after CPT exposure. Dots and error bars (SE) represent gene expression data, lines represent best BMC model. D) BMC accumulation plots of the top 30 responding DDR related genes after CPT exposure. Median BMC were extracted from these plots. $N = 3$.

adaptive to adverse signaling is clearly visible at the highest concentrations. As expected, transcription factor activity analysis revealed TP53 activity for primarily the hiPSCs and to a lesser extend in the other non-dividing models (supplemental table ESM4). The BMC accumulation plot of the 30 TP53 downstream target genes demonstrated that cells with high proliferative potential (hiPSC and HepG2) respond already at lower concentrations of CPT (Fig. 5d), likely related to replicative stress in the proliferating cells caused by CPT-induced DNA damage.

### *3.6. Transcriptomic space of HLCs and other liver test systems in TNFα-mediated inflammatory signaling*

Tumor necrosis factor alpha (TNF) is a natural ligand of p55, TNF receptor I, and involved in the acute phase reaction of the systemic inflammation response. Here, we used TNF to induce an inflammation NF-kB signaling response in our test systems. A PCA analysis on a set of the TNF responsive genes (see ESM2) across all test system showed a very distinct TNF response of the HLCs as compared to PHH, HepG2 and hiPSC (Fig. 6a). For HLCs (and to a lesser extent, HepG2), there was a

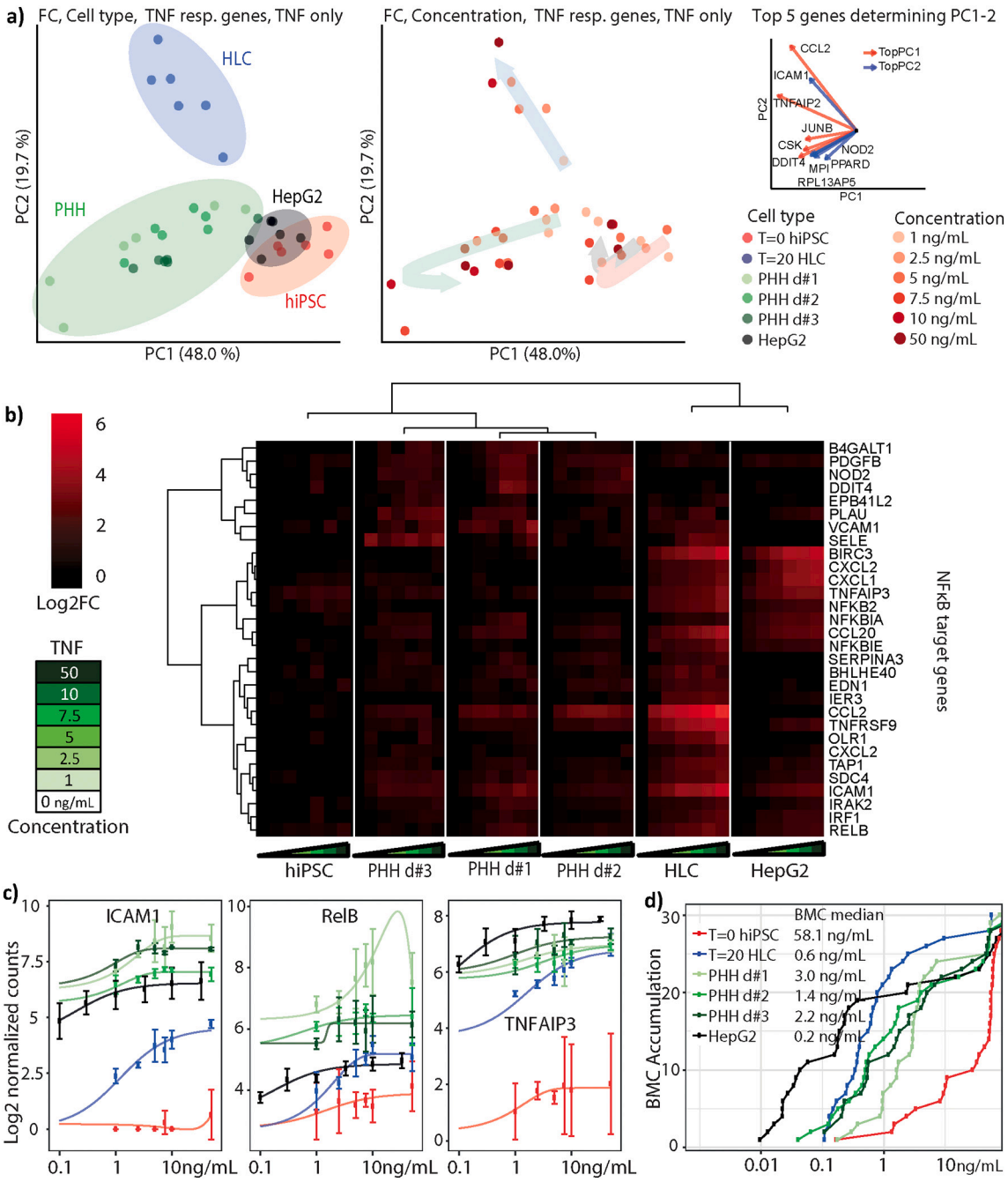


**Fig. 6. Effect of the inflammation response on the transcriptomic space of hiPSC, HLC, PHH and HepG2.** A) Left panel: PCA of the TNF responsive genes (log2 normalized counts) with all treatments. Right panel: PCA of log2 fold changes of the TNF responsive genes after TNF exposure. The vector plots on the right represent the top 5 most determining genes of PC1 (red) or PC2 (blue). The size and orientation of the vector represent the contribution and PC-orientation of the 10 genes. B) Hierarchical clustering of the log2 fold changes of the top 30 NFκB related genes after TNF exposure. C) Concentration response curves of log2 normalized counts for three NFκB target genes after TNF exposure. Dots and error bars (SE) represent gene expression data, lines represent best BMC model. D) BMC accumulation plots of the top 30 responding NFκB related genes after TNF exposure. Median BMC were extracted from these plots. $N = 3$.

concentration-dependent shift along the PC2 axis, mainly caused by increased expression of typical inflammation markers like *TNFAIP2, ICAM1* and *CCL2*. TNF exposure only led to a mild transcriptomic shift in the HepG2 and hiPSC. For PHH, a concentration-dependent shift along the PC1 axis was found which was mostly determined by *JUNB, DDIT4* and *CSK*. These genes are known to play a role in stress response signaling but not necessarily inflammation or NF-κB signaling pathway. The unique TNF response of every model was also evident from the hierarchical clustering of the log2 fold changes of the 30 most responsive NF-κB targets after TNF exposure (Fig. 6b). It was evident that HLCs were by far the most sensitive to TNF exposure, as already at low concentrations a strong upregulation of typical inflammatory genes including *ICAM1, CCL2/20, CXCL1/2, TNFAIP3, CXCL5, VCAM1* and *SOCS3* was seen. Surprisingly, this change was not caused by an increased expression of the TNF-receptor family members. Only expression of *TNFRSF21* (associated with the fetal liver) was significantly increased in the HLCs model as compared to PHH. TNF concentration responses of three proto-typical NF-κB downstream target genes (*ICAM, RELB* and *TNFAIP3*) demonstrated that while the basal expression levels of these genes in HLCs was low, there was a very strong

induction after TNF exposure (Fig. 6c). This effect was virtually absent in the undifferentiated hiPSCs. In HepG2 and PHH, there was higher basal gene expression of inflammatory targets, but only a mild induction after exposure to TNF. Besides, variation was seen in upregulation of inflammatory genes between the different PHHs, where for instance *CCL2* was dose-dependent upregulated in two of the PHHs but not in the third PHHs potentially due to the difference in initial inflammation state. Transcription factor activity analysis showed the activation of various NF-κB subunits among all models except for hiPSCs (supplemental table ESM4). The BMC accumulation plot for the 30 most responsive NF-κB targets indicated that both HepG2 and HLCs were very sensitive towards TNF exposure but hiPSC not at all (Fig. 6d).

## 4. Discussion

PHH are regarded as the gold standard for hepatotoxic liability testing, but suffer from lack of availability, poor in vitro metabolic stability, and variability. Therefore, hiPSC-hepatic progeny is being evaluated as an alternative for chemical safety testing. Given that chemicals cause cell injury that triggers cellular stress response pathways, a question that has yet to be answered is how hiPSC-hepatic progeny compares to PHH in the context of cellular stress response activation. Using transcriptomic approaches, here we systematically assessed four critical stress pathways involved in cell injury repair in hiPSC, hiPSC-HLCs, PHH and HepG2 cells. Our data indicate that the cellular stress response of HLCs is clearly different from undifferentiated hiPSC and more resembles that of liver (PHH and HepG2) cell type responses. The sensitivity score, which was calculated as an EC50 over the stress pathway BMC accumulation plot, was within a 3-fold difference compared to PHH donors, HLCs being more sensitive to oxidative stress and cytokine signaling, and PHH being more sensitive for ER stress.

We found that untreated HLCs were transcriptionally quite distinct from PHH. The overall transcriptomic similarity between HLC and PHH was as close to that of HLC and undifferentiated hiPSC, an observation that was previously also reported by another group (Xu et al., 2018). However, HLCs are remarkably similar to PHH when comparing cellular stress response pathway activation. This suggests that HLCs have gained a differentiation status that reflects the responses observed in PHH. This is consistent with a previous proteomic study that compared the proteomic profiles of HLCs and PHH (Hurrell et al., 2018) and also sensitivity to hepatotoxic drugs (Boon et al., 2020; Kang et al., 2016). This indicates that despite their relative immaturity, HLCs respond similarly to liver toxicants as gold standard in vitro models like PHH. Therefore, at least for compounds that do not require bioactivation, HLCs might be a predictive model for hepatotoxicity.

For this study, we included one model compound per stress pathway to activate either an oxidative stress, DNA damage, ER stress or inflammation conditions. Our study demonstrates clear dose-response differences at the individual gene level between the different cell models. PHH were in particular sensitive for the onset of the UPR genes as a consequence of ER stress when compared to the other models. While the three individual PHH donors showed average BMCs for UPR genes of around 0.1 μM, this was seven times higher for HLCs. Overall, individual UPR genes were activated throughout all model systems, although at different concentration levels. *HERPUD1*, *DDIT3* and *HSPA5*, three bona fide UPR genes, were already activated at around 0.1 μM in PHH being most sensitive, while HLCs showed activation starting at 1 μM. Despite difference in sensitivity, HLCs showed in general higher upregulation of UPR specific genes compared to PHH. The UPR is of prominent importance in both DILI responses in PHH as well as in the rat liver in vivo (Fredriksson et al., 2014) and in liver disease settings (Lebeaupin et al., 2018).

In contrast to the UPR pathway, HLCs were more sensitive to TNF-mediated NF-kB target gene expression than the three PHH donors and more comparable to HepG2 cells. Clearly, differentiated HLCs were distinct from hiPSCs, as only very minimal TNF-mediated NF-kB target gene activation was observed in hiPSCs. As various liver diseases involve inflammatory signaling through NF-kB, including non-alcoholic fatty liver disease (NAFLD), liver fibrosis and cancer (Brenner et al., 2013) as well as DILI (Fredriksson et al., 2011), HLCs can be a good model to study TNF-mediated signaling responses, although this does not reflect the multicellular system including Kupffer and stellate cells mediating inflammatory signaling. If HLCs are combined with multiple liver-specific cell types in a 3D structure, this may further improve its relevance for the study of inflammatory signaling (Ouchi et al., 2019). The limited sensitivity of the PHH to TNF could be related to the prior disease status, and that for instance the colon metastases had already affected the level of local or systemic cytokine levels that influence the PHH prior to isolation. On top of that, it is likely that the hepatocyte harvesting method also contributes to a pre-inflammatory state of the PHH.

Similarly, HLCs were also more sensitive for DEM-induced oxidative stress compared to PHH, and even more so than hiPSCs and HepG2, which showed an 8-fold lower sensitivity for NRF2 target gene induction. A study by Kang et al. showed similar differences where HLCs were more comparable to PHH in oxidative stress induction by acetaminophen than the less sensitive HepG2 model (Kang et al., 2016). In the liver, high metabolic activity of hepatocytes results in elevated levels of ROS due to biotransformation and xenobiotic metabolism and therefore the necessity of a cellular defense mechanism through strong activation of the NRF2-mediated anti-oxidant response (Marí et al., 2010). In that respect, the differentiation of hiPSCs towards HLCs lead to a sensitivity towards oxidative stress comparable to PHH making them suitable for the evaluation of chemical-induced oxidative stress response signaling.

On the other hand, HLCs were the least sensitive cell type for CPT-induced DDR-mediated TP53 activation. While for all three PHH donors, the activation of TP53 target genes, such as *MDM2*, *CDKN1A* and *BTG2* was initiated at around 10 μM, in HLCs this was about 2 times higher. These HLC responses are in sharp contrast to the high sensitivity of undifferentiated hiPSCs, responding already at 3 μM, and therefore illustrates the strong difference of the DDR in hiPSCs and differentiated liver progeny. Indeed, a study by Shimada et al. showed strong sensitivity towards DNA damage in hiPSCs compared to a differentiated state indicating a shift in the regulatory network of DNA damage signaling during differentiation (Shimada et al., 2019).

Sensitivity towards the analyzed stress pathways is an important feature for a hepatotoxicity model. We believe that in this respect a model cannot be too sensitive. Especially for DNA damage as a mutagenic effect will always increase the chance for a malignancy and sensitive models have in this respect less false negatives. For the in vitro to in vivo translation, the retrieved BMCs should be benchmarked to the BMCs of compounds of which the pathological outcome is known. Besides stress pathway sensitivity, metabolism is another important feature for a hepatotoxicity model. HepG2 cells as cultured in a 2D monolayer have a very low phase I and phase II drug metabolism. Bioconversion characteristics can therefore not be studied in this simple model (Hiemstra et al., 2019), and PHHs and HLCs are in this case the preferred model.

In conclusion, despite limitation in full hepatocyte maturation, which caused a quite distinct overall basal transcriptomic space of HLC in comparison to PHH, HLCs did gain specific adaptive cellular stress response networks that mimic those of PHHs. We envision that the use of HLCs in hepatotoxicity screening will steadily increase and when differentiation protocols are further optimized, HLCs might be more reliable to uncover stress response activation to assess chemical safety as well as to understand the modulation of cellular stress responses in hiPSC-derived liver disease models.

## Declaration of Competing Interest

Lysiane Richert is founder and CSO of KaLy-Cell.

## Acknowledgments

This work was supported by the EU-ToxRisk project funded by the European Union's Horizon 2020 programme (grant agreement number 681002), the Belgium IWT project HILIM-3D (project 140045) and the IMI MIP-DILI project (grant agreement number 115336).

## Appendix A. Supplementary data

Supplementary data to this article can be found online at https://doi.org/10.1016/j.tiv.2021.105107.

## References

Acikgöz, A., Giri, S., Cho, M.G., Bader, A., 2013. Morphological and functional analysis of hepatocyte spheroids generated on poly-HEMA-treated surfaces under the influence of fetal calf serum and nonparenchymal cells. Biomolecules 3, 242–269. https://doi.org/10.3390/biom3010242.

Boon, R., Kumar, M., Elia, I., Ordovas, L., Jacobs, F., One, J., De Smedt, J., Eelen, G., Bird, M., Roelandt, P., Rossi, M., Tricot, T., Aguire-Vazquez, M., Vanwelden, T., Chesnais, F., El Taghdouini, A., Najimi, M., Sokal, E., Cassiman, D., Hu, W.-S., Snoeys, J., Monschouwer, M., Lange, C., Carmeliet, Peter, Fendt, S.-M., Verfaillie, C., De Smedt, J., Aguirre-Vazquez, M., Vanwelden, T., Chesnais, F., El Taghdouini, A., Sokal, E., Cassiman, D., Lange, C., Carmeliet, Pieter, Fendt, S.M., Verfaillie, C.M., 2020. Amino acid levels determine metabolism and CYP450 function of stem cell derived hepatocytes and hepatoma cell lines. Nat. Metab. 1–16 https://doi.org/10.1038/s41467-020-15058-6.

Brenner, C., Galluzzi, L., Kepp, O., Kroemer, G., 2013. Decoding cell death signals in liver inflammation. J. Hepatol. https://doi.org/10.1016/j.jhep.2013.03.033.

Czysz, K., Minger, S., Thomas, N., 2015. Dmso efficiently down regulates pluripotency genes in human embryonic stem cells during definitive endoderm derivation and increases the proficiency of hepatic differentiation. PLoS One 10, 1–16. https://doi.org/10.1371/journal.pone.0117689.

Dowle, M., Srinivasan, A., Gorecki, J., 2016. data. table: Extension of 'data. frame'. URL https://CRAN. R-project. org/package= data. table.

Fredriksson, L., Herpers, B., Benedetti, G., Matadin, Q., Puigvert, J.C., de Bont, H., Dragovic, S., Vermeulen, N.P.E., Commandeur, J.N.M., Danen, E., De Graauw, M., van de Water, B., 2011. Diclofenac inhibits tumor necrosis factor-α-induced nuclear factor-κB activation causing synergistic hepatocyte apoptosis. Hepatology 53, 2027–2041. https://doi.org/10.1002/hep.24314.

Fredriksson, L., Wink, S., Herpers, B., Benedetti, G., Hadi, M., De Bont, H., Groothuis, G., Luijten, M., Danen, E., De Graauw, M., Meerman, J., van de Water, B., 2014. Drug-induced endoplasmic reticulum and oxidative stress responses independently sensitize toward TNFα-mediated hepatotoxicity. Toxicol. Sci. 140, 144–159. https://doi.org/10.1093/toxsci/kfu072.

Gao, X., Liu, Y., 2017. A transcriptomic study suggesting human iPSC-derived hepatocytes potentially offer a better in vitro model of hepatotoxicity than most hepatoma cell lines. Cell Biol. Toxicol. 33, 407–421. https://doi.org/10.1007/s10565-017-9383-z.

Garcia-Alonso, L., Iorio, F., Matchan, A., Fonseca, N., Jaaks, P., Peat, G., Pignatelli, M., Falcone, F., Benes, C.H., Dunham, I., Bignell, G., McDade, S.S., Garnett, M.J., Saez-Rodriguez, J., 2018. Transcription factor activities enhance markers of drug sensitivity in cancer. Cancer Res. 78, 769–780. https://doi.org/10.1158/0008-5472.CAN-17-1679.

Ghosheh, N., Olsson, B., Edsbagge, J., Küppers-Munther, B., Van Giezen, M., Asplund, A., Andersson, T.B., Björquist, P., Carén, H., Simonsson, S., Sartipy, P., Synnergren, J., 2016. Highly synchronized expression of lineage-specific genes during in vitro hepatic differentiation of human pluripotent stem cell Lines. Stem Cells Int. 2016. https://doi.org/10.1155/2016/8648356.

Godoy, P., Schmidt-Heck, W., Natarajan, K., Lucendo-Villarin, B., Szkolnicka, D., Asplund, A., Björquist, P., Widera, A., Stöber, R., Campos, G., Hammad, S., Sachinidis, A., Chaudhari, U., Damm, G., Weiss, T.S., Nüssler, A., Synnergren, J., Edlund, K., Küppers-Munther, B., Hay, D.C., Hengstler, J.G., 2015. Gene networks and transcription factor motifs defining the differentiation of stem cells into hepatocyte-like cells. J. Hepatol. 63, 934–942. https://doi.org/10.1016/j.jhep.2015.05.013.

Helsen, N., Debing, Y., Paeshuyse, J., Dallmeier, K., Boon, R., Coll, M., Sancho-Bru, P., Claes, C., Neyts, J., Verfaillie, C.M., 2016. Stem cell-derived hepatocytes: a novel model for hepatitis e virus replication. J. Hepatol. 64, 565–573. https://doi.org/10.1016/j.jhep.2015.11.013.

Hiemstra, S., Ramaiahgari, S.C., Wink, S., Callegaro, G., Coonen, M., Meerman, J., Jennen, D., van den Nieuwendijk, K., Dankers, A., Snoeysde Bont, J.H., 2019. High-throughput confocal imaging of differentiated 3D liver-like spheroid cellular stress response reporters for identification of drug-induced liver injury liability. Arch. toxicol. 93, 2895–2911. https://doi.org/10.1007/s00204-019-02552-0.

Hurrell, T., Segeritz, C.-P., Vallier, L., Lilley, K., Cromarty, A.D., 2018. Proteomic responses of HepG2 cell monolayers and 3D spheroids to selected Hepatotoxins. Toxicol Sc 164, 229–239. https://doi.org/10.1093/toxsci/kfy084/4960110.

José, M., Lechón, G., Tolosa, L., 2016. Human hepatocytes derived from pluripotent stem cells : a promising cell model for drug hepatotoxicity screening. Arch. Toxicol. 90, 2049–2061. https://doi.org/10.1007/s00204-016-1756-1.

Kadota, K., Nishimura, S.-I., Bono, H., Nakamura, S., Hayashizaki, Y., Okazaki, Y., Takahashi, K., 2015. Detection of genes with tissue-specific expression patterns using Akaike's information criterion procedure. Physiol. Genomics 12, 251–259. https://doi.org/10.1152/physiolgenomics.00153.2002.

Kang, S.J., Lee, H.M., Park, Y. Il, Yi, H., Lee, H., So, B.J., Song, J.Y., Kang, H.G., 2016. Chemically induced hepatotoxicity in human stem cell-induced hepatocytes compared with primary hepatocytes and HepG2. Cell Biol. Toxicol. 32, 403–417. https://doi.org/10.1007/s10565-016-9342-0.

Kaur, P., Kalia, S., Bansal, M.P., 2006. Effect of diethyl maleate induced oxidative stress on male reproductive activity in mice: redox active enzymes and transcription factors expression. Mol. Cell. Biochem. 291, 55–61. https://doi.org/10.1007/s11010-006-9195-6.

Kolde, R., 2012. Pheatmap: Pretty Heatmaps. R Packag. version 61.

Kritsch, D., Hoffmann, F., Steinbach, D., Jansen, L., Mary Photini, S., Gajda, M., Mosig, A. S., Sonnemann, J., Peters, S., Melnikova, M., Thomale, J., Dürst, M., Runnebaum, I. B., Häfner, N., 2017. Tribbles 2 mediates cisplatin sensitivity and DNA damage response in epithelial ovarian cancer. Int. J. Cancer 141, 1600–1614. https://doi.org/10.1002/ijc.30860.

Kullak-Ublick, G.A., Andrade, R.J., Merz, M., End, P., Benesic, A., Gerbes, A.L., Aithal, G. P., 2017. Drug-induced liver injury: recent advances in diagnosis and risk assessment. Gut 66, 1154–1164. https://doi.org/10.1136/gutjnl-2016-313369.

Lebeaupin, C., Vallée, D., Hazari, Y., Hetz, C., Chevet, E., Bailly-Maitre, B., 2018. Endoplasmic reticulum stress signalling and the pathogenesis of non-alcoholic fatty liver disease. J. Hepatol. https://doi.org/10.1016/j.jhep.2018.06.008.

Li, S., Guo, J., Ying, Z., Chen, S., Yang, L., Chen, K., Long, Q., Qin, D., Pei, D., Liu, X., 2015. Valproic acid-induced hepatotoxicity in alpers syndrome is associated with mitochondrial permeability transition pore opening-dependent apoptotic sensitivity in an induced pluripotent stem cell model. Hepatology 61, 1730–1739. https://doi.org/10.1002/hep.27712.

Liguori, M.J., Anderson, M.G., Bukofzer, S., McKim, J., Pregenzer, J.F., Retief, J., Spear, B.B., Waring, J.F., 2005. Microarray analysis in human hepatocytes suggests a mechanism for hepatotoxicity induced by trovafloxacin. Hepatology 41, 177–186. https://doi.org/10.1002/hep.20514.

Love, M.I., Huber, W., Anders, S., 2014. Moderated estimation of fold change and dispersion for RNA-seq data with DESeq2. Genome Biol. 15, 1–21. https://doi.org/10.1186/s13059-014-0550-8.

Lu, J., Einhorn, S., Venkatarangan, L., Miller, M., Mann, D.A., Watkins, P.B., LeCluyse, E., 2015. Morphological and functional characterization and assessment of iPSC-derived hepatocytes for in vitro toxicity testing. Toxicol. Sci. 147, 39–54. https://doi.org/10.1093/toxsci/kfv117.

Lundquist, P., Lööf, J., Sohlenius-Sternbeck, A.K., Floby, E., Johansson, J., Bylund, J., Hoogstraate, J., Afzelius, L., Andersson, T.B., 2014. The impact of solute carrier (SLC) drug uptake transporter loss in human and rat cryopreserved hepatocytes on clearance predictions. Drug Metab. Dispos. 42, 469–480. https://doi.org/10.1124/dmd.113.054676.

Marí, M., Colell, A., Morales, A., Von Montfort, C., Garcia-Ruiz, C., Fernández-Checa, J. C., 2010. Redox control of liver function in health and disease. Antioxid. Redox Signal. https://doi.org/10.1089/ars.2009.2634.

Mav, D., Shah, R.R., Howard, B.E., Auerbach, S.S., Bushel, P.R., Collins, J.B., Gerhold, D. L., Judson, R.S., Karmaus, A.L., Maull, E.A., Mendrick, D.L., Merrick, B.A., Sipes, N. S., Svoboda, D., Paules, R.S., 2018. A hybrid gene selection approach to create the S1500+ targeted gene sets for use in high-throughput transcriptomics. PLoS One 13, 1–19. https://doi.org/10.1371/journal.pone.0191105.

Ouchi, R., Togo, S., Kimura, M., Shinozawa, T., Koido, M., Koike, H., Thompson, W., Karns, R.A., Mayhew, C.N., McGrath, P.S., McCauley, H.A., Zhang, R.R., Lewis, K., Hakozaki, S., Ferguson, A., Saiki, N., Yoneyama, Y., Takeuchi, I., Mabuchi, Y., Akazawa, C., Yoshikawa, H.Y., Wells, J.M., Takebe, T., 2019. Modeling steatohepatitis in humans with pluripotent stem cell-derived organoids. Cell Metab. 30, 374–384 e6. https://doi.org/10.1016/j.cmet.2019.05.007.

Pagès, H., Carlson, M., Falcon, S., Li, N., 2018. AnnotationDbi: Annotation Database Interface. R Packag. version 1.43.1.

Phillips, J.R., Svoboda, D.L., Tandon, A., Patel, S., Sedykh, A., Mav, D., Kuo, B., Yauk, C. L., Yang, L., Thomas, R.S., Gift, J.S., Allen Davis, J., Olszyk, L., Alex Merrick, B., Paules, R.S., Parham, F., Saddler, T., Shah, R.R., Auerbach, S.S., 2019. BMD express 2: enhanced transcriptomic dose-response analysis workflow. Bioinformatics 35, 1780–1782. https://doi.org/10.1093/bioinformatics/bty878.

Ramaiahgari, S.C., Auerbach, S.S., Saddler, T.O., Rice, J.R., Dunlap, P.E., Sipes, N.S., Devito, M.J., Shah, R.R., Bushel, P.R., Merrick, B.A., Paules, R.S., Ferguson, S.S., 2019. The power of resolution: contextualized understanding of biological responses to liver injury chemicals using high-throughput transcriptomics and benchmark concentration modeling. Toxicol. Sci. 169, 553–566. https://doi.org/10.1093/toxsci/kfz065.

Shimada, M., Tsukada, K., Kagawa, N., Matsumoto, Y., 2019. Reprogramming and differentiation-dependent transcriptional alteration of DNA damage response and apoptosis genes in human induced pluripotent stem cells. J. Radiat. Res. 60, 719–728. https://doi.org/10.1093/jrr/rrz057.

Sison, R.L., Volker, Y., Esther, M.L., Eliane, J., Antherieu, S., Aerts, H., Gerets, H.H.J., Labbe, G., Hoët, D., Dorau, M., Schofield, C.A., Lovatt, C.A., Jones, R.P., Elmasry, M., Weaver, R.J., Hewitt, P.G., 2017. Organ toxicity and mechanisms: a multicenter assessment of single - cell models aligned to standard measures of cell health for prediction of acute hepatotoxicity. Arch. Toxicol. 91, 1385–1400. https://doi.org/10.1007/s00204-016-1745-4.

Takahashi, K., Tanabe, K., Ohnuki, M., Narita, M., Ichisaka, T., Tomoda, K., Yamanaka, S., 2007. Induction of pluripotent stem cells from adult human fibroblasts by defined factors. Cell 131, 861–872. https://doi.org/10.1016/j.cell.2007.11.019.

Tricot, T., Helsen, N., Kaptein, S.J.F., Neyts, J., Verfaillie, C.M., 2018. Human stem cell-derived hepatocyte-like cells support Zika virus replication and provide a relevant model to assess the efficacy of potential antivirals. PLoS One 13, 1–17. https://doi.org/10.1371/journal.pone.0209097.

Wang, H., Wang, X., Ke, Z.J., Comer, A.L., Xu, M., Frank, J.A., Zhang, Z., Shi, X., Luo, J., 2015. Tunicamycin-induced unfolded protein response in the developing mouse brain. Toxicol. Appl. Pharmacol. 283, 157–167. https://doi.org/10.1016/j.taap.2014.12.019.

Weaver, R.J., Blomme, E.A., Chadwick, A.E., Copple, I.M., Gerets, H.H.J., Goldring, C.E., Guillouzo, A., Hewitt, P.G., Ingelman-Sundberg, M., Jensen, K.G., Juhila, S., Klingmüller, U., Labbe, G., Liguori, M.J., Lovatt, C.A., Morgan, P., Naisbitt, D.J., Pieters, R.H.H., Snoeys, J., van de Water, B., Williams, D.P., Park, B.K., 2019. Managing the challenge of drug-induced liver injury: a roadmap for the development and deployment of preclinical predictive models. Nat. Rev. Drug Discov. 19, 131–148. https://doi.org/10.1038/s41573-019-0048-x.

Wickham, H., 2009. ggplot2: Elegant Graphics for Data Analysis. Springer-Verlag, New York.

Wickham, H., 2011. The Split-apply-combine strategy for data analysis. J. Stat. Softw. 40. Doi:10.18637/jss.v040.i01.

Wickham, H., Henry, L., 2018. Tidyr: Easily Tidy Data with “spread” and “gather” Functions. R Packag. version 0.8.0. https//CRAN.R-project.org/package=tidyr.

Wink, S., Hiemstra, S., Huppelschoten, S., Danen, E., Hendriks, G., Vrieling, H., Herpers, B., van de Water, B., 2014. Quantitative high content imaging of cellular adaptive stress response pathways in toxicity for chemical safety assessment quantitative high content imaging of cellular adaptive stress response pathways in division of toxicology, leiden academic centre f. Chem. Res. Toxicol. 27, 338–355. https://doi.org/10.1021/tx4004038.

Wink, S., Hiemstra, S.W., Huppelschoten, S., Klip, J.E., van de Water, B., 2018. Dynamic imaging of adaptive stress response pathway activation for prediction of drug induced liver injury. Arch. Toxicol. 92, 1797–1814. https://doi.org/10.1007/s00204-018-2178-z.

Xu, Z., He, X., Shi, X., Xia, Y., Liu, X., Wu, H., Li, P., Zhang, H., Yin, W., Du, X., Li, L., Li, Y., 2018. Analysis of differentially expressed genes among human hair follicle-derived iPSCs, induced hepatocyte-like cells, and primary hepatocytes. Stem Cell Res Ther 9. https://doi.org/10.1186/s13287-018-0940-z.

Yeakley, J.M., Shepard, P.J., Goyena, D.E., Vansteenhouse, H.C., McComb, J.D., Seligmann, B.E., 2017. A Trichostatin a expression signature identified by TempO-Seq targeted whole transcriptome profiling. PLoS One 12. https://doi.org/10.1371/journal.pone.0178302.

Zhang, Z., 2016. Reshaping and aggregating data: an introduction to reshape package. Ann. Transl. Med. 4, 78. https://doi.org/10.3978/j.issn.2305-5839.2016.01.33.